Ivan Komar
Nenad Vulić
Liane Roldo

ISSN 1333-1124

HYDRODYNAMIC AND ELASTOHYDRODYNAMIC LUBRICATION MODEL TO VERIFY THE PERFORMANCE OF MARINE PROPULSION SHAFTING

UDC 24.977

Summary

Hydrodynamic and elastohydrodynamic lubrication models were applied to compare the performance of oil lubricated metallic journal bearings with that of sea water lubricated polymer journal bearings in ship propulsion systems. A numerical model based upon the finite difference method and an isoviscous model, together with a computer program with two modules have been used to evaluate the process parameters. The method and model calculations were tested using the data collected from two different types of actual vessels in service. Regarding the stern tube journal bearings, results indicate that the developed software applications attain high approximation accuracy regardless of the relatively simple numerical model.

Key words: *stern tube bearing, hydrodynamic, elastohydrodynamic, journal bearing, water lubricated*

1. Introduction

Ship propeller shaft stern tube bearings are traditionally made of white metal and are oil lubricated. An alternative solution may be provided by water lubricated polymer bearings instead of white metal ones, offering some very important benefits. First of all, sea water lubricated polymer bearings generate a significantly smaller amount of heat loss due to hydrodynamic friction for the same running condition (loading and shaft speed) compared to white metal bearings. This means a smaller effective power loss and consequently fuel savings. Furthermore, water lubricated shaft line bearings are also practically maintenance free and would certainly represent a *green* solution, because the risk of oil leakage is avoided [1].

Stern tube journal bearings operate with hydrodynamic lubrication (HL), in which the lubricant film generated by journal rotation separates the bearing surface from the journal surface.

This model and its evaluation by means of finite difference method correctly describe the lubrication of white metal bearings. However, in polymer bearings, due to material elastic deformation, the elastohydrodynamic lubrication (EHL) model is to be applied [2,3].

The paper aims at describing possibilities of the application of a hydrodynamic and an elastohydrodynamic lubrication model to ship stern tube bearings. Calculation programs have been prepared in the form of a spreadsheet with a programmable background. Oil lubricated white metal journal bearings and water lubricated polymer ones, implemented in actual ship propulsion systems, were the basis for the case study, calculation model verification and validation. Power loss and other performance characteristics have been analysed.

2. Model formulation

2.1 Hydrodynamic lubrication (HL) journal bearing model

Assuming that η = constant, the Reynolds equation describes the lubricant pressure distribution in a journal bearing as a function of the journal speed, bearing geometry, and lubricant viscosity in stationary hydrodynamic lubrication in the journal bearing [2,3]:

$$\frac{\partial}{\partial x}\left(h^3\frac{\partial p}{\partial x}\right)+\frac{\partial}{\partial y}\left(h^3\frac{\partial p}{\partial y}\right)=6v_j\eta\frac{\partial h}{x} \tag{1}$$

The Reynolds equation can be numerically solved by means of finite difference methods. To solve the Reynolds equation (expressed in terms of film thickness h, pressure p, journal velocity v_j, and lubricant dynamic viscosity η) using this method, the equation is to be transformed into the following dimensionless form [2]:

$$\frac{\partial}{\partial \tilde{x}}\left(\tilde{h}^3\frac{\partial \tilde{p}}{\partial \tilde{x}}\right)+\left(\frac{R_B}{L}\right)^2\frac{\partial}{\partial \tilde{y}}\left(\tilde{h}^3\frac{\partial \tilde{p}}{\partial \tilde{y}}\right)=\frac{\partial \tilde{h}}{\partial \tilde{x}} \tag{2}$$

with the non-dimensional variables:

$$\tilde{h}=h/c\,;\ \tilde{x}=x/R_B\,;\ \tilde{y}=y/L\,;\ \tilde{p}=pc^2/6v_j\eta R_B \tag{3}$$

To improve the accuracy of numerical solutions of the Reynolds equation, the Vogelpohl parameter is introduced as follows:

$$M_v=\tilde{p}\cdot\tilde{h}^{1.5} \tag{4}$$

Substitution into the non-dimensional form of the Reynolds equation (2) yields the Vogelpohl equation, to which the finite difference method is implemented [2]:

$$\frac{\partial^2 M_v}{\partial \tilde{x}^2}+\left(\frac{R_B}{L}\right)^2\frac{\partial^2 M_v}{\partial \tilde{y}^2}=F_vM_v+G \tag{5}$$

with the Vogelpohl parameters F_v and G for journal bearings defined as follows [2]:

$$F_v=\frac{0.75\left[\left(\frac{\partial \tilde{h}}{\partial \tilde{x}}\right)^2+\left(\frac{R}{L}\right)^2\left(\frac{\partial \tilde{h}}{\partial \tilde{y}}\right)^2\right]}{\tilde{h}^2}+\frac{1.5\left[\frac{\partial^2 \tilde{h}}{\partial \tilde{x}^2}+\left(\frac{R}{L}\right)^2\frac{\partial^2 \tilde{h}}{\partial \tilde{y}^2}\right]}{\tilde{h}}\quad\text{and}\quad G=\frac{\left(\frac{\partial \tilde{h}}{\partial \tilde{x}}\right)}{\tilde{h}^{1.5}}$$

Frictional force developed in the lubricant hydrodynamic film is calculated by integrating the shear stress over the bearing area as follows:

$$F_t=\int_0^L\int_0^{2\pi R_B}\tau\,dx\,dy \tag{6}$$

where the shear stress is expressed as follows:

$$\tau = \frac{\eta v_j}{h} + \frac{h}{2}\frac{dp}{dx} \tag{7}$$

Transformation of the frictional force into a non-dimensional form can be done by inserting the non-dimensional variables (3) into shear stress (7), thus obtaining:

$$\tau = \frac{\eta v_j}{c}\frac{1}{\tilde{h}} + \frac{c\tilde{h}}{2}\frac{6v_j\eta R_B}{c^2}\frac{1}{R_B}\frac{d\tilde{p}}{d\tilde{x}} = \left(\frac{v_j\eta}{c}\right)\left(\frac{1}{\tilde{h}} + 3\tilde{h}\frac{d\tilde{p}}{d\tilde{x}}\right) \tag{8}$$

Inserting for x and y from equations (3) yields:

$$\tau dxdy = \tau d\tilde{x}d\tilde{y}R_B L \tag{9}$$

Frictional force in terms of non-dimensional quantities is obtained by inserting (8) and (9) into (6):

$$F_t = \int_0^L \int_0^{2\pi R_B} \tau dxdy = R_B L \int_0^1 \int_0^{2\pi} \tau d\tilde{x}d\tilde{y} = \frac{R_B L \eta v_j}{c}\int_0^1 \int_0^{2\pi}\left(\frac{1}{\tilde{h}} + 3\tilde{h}\frac{d\tilde{p}}{d\tilde{x}}\right)d\tilde{x}d\tilde{y} \tag{10}$$

Obviously, from (10), the non-dimensional shear stress is expressed as [2]:

$$\tilde{\tau} = \frac{1}{\tilde{h}} + 3\tilde{h}\frac{d\tilde{p}}{d\tilde{x}} \tag{11}$$

so the equation (10) can be rewritten in the following form:

$$F_t = \frac{R_B L \eta v_j}{c}\int_0^1 \int_0^{2\pi} \tilde{\tau} d\tilde{x}d\tilde{y} = \tilde{F}_t\left(\frac{R_B L \eta v_j}{c}\right) \tag{12}$$

Friction coefficient in journal bearings is the ratio of the circumferential friction force to the bearing radial load [2]:

$$\mu = \frac{F_t}{F_r} = \frac{\int_0^L \int_0^{2\pi R_B} \tau dxdy}{\int_0^L \int_0^{2\pi R_B} pdxdy} \tag{13}$$

A similar quantity is defined by dividing the dimensionless friction by the dimensionless load. Radial load on a journal bearing is expressed as:

$$F_r = \int_0^L \int_0^{2\pi R_B} -\cos(\tilde{x})pdxdy \tag{14}$$

The term *-cos*($\tilde{x}$) arises from the fact that the load supporting pressure is located close to $\tilde{x}$ = π *or cos*($\tilde{x}$) = -1. Expressing equation (14) in terms of nondimensional quantities gives:

$$F_r = \left(\frac{6v_j\eta R_B}{c^2}\right)R_B L \int_0^1 \int_0^{2\pi} -\cos(\tilde{x})\tilde{p}d\tilde{x}d\tilde{y} = \tilde{F}_r\left(\frac{6R_B{}^2 L v_j \eta}{c^2}\right) \tag{15}$$

Inserting (12) and (15) into (13) gives the expression for the coefficient of friction:

$$\mu = \frac{F_t}{F_r} = \frac{\left(\dfrac{R_B L \eta v_j}{c}\right)}{\left(\dfrac{6 R_B^{\,2} L v_j \eta}{c^2}\right)} \frac{\tilde{F}_t}{\tilde{F}_r} = \left(\frac{c}{6R_B}\right)\left(\frac{\tilde{F}_t}{\tilde{F}_r}\right) \tag{16}$$

Hence

$$\frac{\tilde{F}_t}{\tilde{F}_r} = \left(\frac{6R_B}{c}\right)\mu \tag{17}$$

Misalignment and cavitation have been disregarded supposing an ideally aligned journal.

2.2 Elastohydrodynamic (EHL) lubrication model

When the elastic deformation of the interacting surfaces plays an important role, it is necessary to apply a different model, such as the elastohydrodynamic lubrication model (EHL).

The magnitude of elastic deformation and changes in lubricant viscosity depend mostly on the applied load and Young's modulus of the material [3,4,5].

Calculation of the bearing elastic deformation is based on the Hamrock and Dowson elastohydrodynamic lubrication analysis of isoviscous-elastic body lubrication regimes. In the isoviscous-elastic regime of EHL, elastic deformations of surfaces in contact make a considerable contribution to the thickness of the generated film. The lubricant film pressures are either too low to raise the lubricant viscosity or the lubricant viscosity is relatively insensitive to the pressure. A typical example of such a lubricant is water. This regime is typically found between solids in contact with low Young's modulus, such as a polymeric material [4,5]. In this case, the geometry of the contact area between the journal and the polymer bearing is circumscribed by a narrow rectangle (Fig. 1). Expressions for significant parameters of EHL shown in Table 1 accompanied with the related geometry form of the contact area between the journal and the bearing have been implemented.

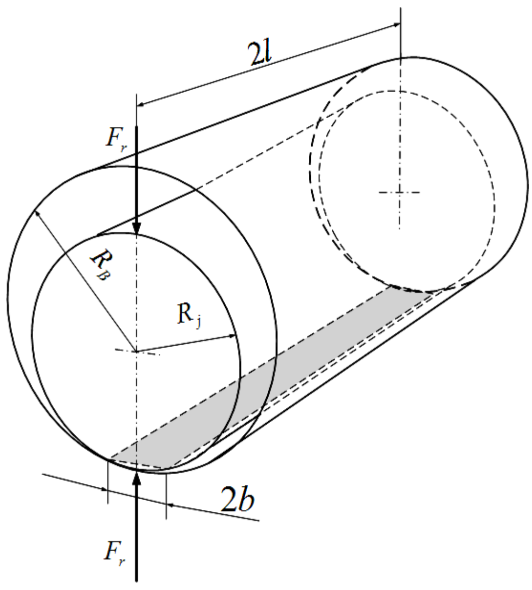

Fig. 1 Geometry of the contact area between the journal and the bearing

Table 1 Expressions for significant parameters of EHL [2,3,6]

No.	*Description*	*Formula*
1.	Reduced radius of curvature (bearing/journal)	$R_{red} = R_B \cdot R_j / (R_B - R_j)$ [m]
2.	Contact area half-length	$a = L/2$ [m]
3.	Contact area half-width	$b = \left[(8F_r L)/(\pi R_{red} E_{red})\right]^{1/2}$ [m]
4.	Non-dimensional ellipticity parameter	$k = a / b$
5.	Reduced Young's modulus	$E_{red} = 2 / \left[(1-\upsilon_B^{\;2})/E_B + (1-\upsilon_j^{\;2})/E_j\right]$
6.	Non-dimensional load parameter	$W = Fr / E_{red} \cdot R^2_{red}$
7.	Non-dimensional minimal film thickness	$\tilde{H}_{\mathrm{min}} = 8{,}7 G_{\mathrm{E}}^{\;0.67}\left(1-0{,}85\mathrm{e}^{-0.31\mathrm{k}}\right)\left(U_{\mathrm{red}}/W\right)^2$
8.	Non-dimensional central film thickness	$\tilde{H}_{\mathrm{c}} = 11{,}15 G_{\mathrm{E}}^{\;0.67}\left(1-0{,}72\mathrm{e}^{-0.28\mathrm{k}}\right)\left(U_{\mathrm{red}}/W\right)^2$
9.	Non-dimensional speed parameter	$U_{red} = v_j \, \eta / E_{red} \, R_{red}$
10.	Non-dimensional elasticity parameter	$G_E = W^{8/3} / U^2_{red}$
11.	Minimal lubricant film thickness	$h_{\mathrm{min}} = \tilde{H}_{\mathrm{min}} R_{red}$ [m]
12.	Central lubricant film thickness	$h_c = \tilde{H}_{\mathrm{c}} R_{red}$ [m]
13.	Effective lubricant film thickness	$h_{eff} = (h_{\mathrm{min}} + h_c)/2$ [m]
14.	Theoretical eccentricity ratio at minimal lubricant film thickness	$\varepsilon_{\mathrm{max}} = 1 - h_{\mathrm{min}} / c$
15.	Theoretical eccentricity ratio at central lubricant film thickness	$\varepsilon_c = 1 - h_c / c$
16.	Effective diameter of deformed bearing	$D_{Beff} = D_B + 2h_{eff}$ [m]
17.	Effective diametrical clearance of deformed bearing	$Z_{eff} = D_{Beff} - D_j$ [m]
18.	Mean effective eccentricity ratio	$\varepsilon_{eff} = 1 - 2h_{eff} / Z_{eff}$
19.	Power loss in the bearing	$P_{loss} = \mu F_r v_j$ [W]
20.	Lubricant flow rate resulting from the development of internal pressure	$Q_1 = D_B^{\;3} \cdot \psi \cdot \omega \cdot q_1$ [m^3/s] $q_1 = f(\varepsilon,\ L/D_B, \Omega = 360^o)$
21.	Lubricant flow rate resulting from the lubricant feeding pressure	$Q_2 = \left[(D_B^{\;3} \cdot \psi \cdot p_E)/\eta)\right] \cdot q_2$ [m^3/s] $q_2 = f(\varepsilon,\ L/D_B, \Omega = 360^o)$
22.	The total lubricant flow rate	$Q = Q_1 + Q_2$ [m^3/s]
23.	Frictional power in a bearing or the amount of heat generated (power loss)	$P_{th} = \rho \cdot c_v \cdot Q \cdot \left(T_{out} - T_{in}\right)$ [W]

Lubricant fed to the bearings forms a film of lubricant separating the sliding surfaces. Owing to the pressure development in the film, the lubricant is forced out of the bearing ends. This is the proportion Q_1 of the lubricant flow rate resulting from the development of internal pressure [6].

In addition to this, there is a flow of lubricant in the circumferential direction through the narrowest clearance gap into the diverging pressure-free gap. As a result of the lubricant feed pressure p_E, an additional amount of lubricant is forced out of the ends of the bearing. This is the proportion Q_2 of the lubricant flow rate resulting from feed pressure [6].

3. Software description, verification and validation data

The developed software consists of two modules: *S11partialRJB* and *S11isoviscRJB* [7].

The first (HL) module was used for a radial journal bearing of a relative length of $1/3 \leq \lambda \leq 3$ [2]. It is based upon a numerical solution of Reynold's equation by the finite difference method, starting from the bearing dimensions, lubricant properties, and loading. The core of numerical calculation (finite difference methods for the numerical solution of Reynold's equation) is the MatLab program *Partial* described in [2]. The program calculates non-dimensional values (relative eccentricity, attitude angle, dimensionless radial bearing load, Petroff multiplier, and maximal dimensionless pressure), as well as essential dimensional values (radial load, frictional force, power loss, etc.). For comparison, the program also calculates relevant values based on analytical formulae from the standard DIN 31652-2:1983[6], with a warning regarding their applicability when necessary. Calculation of relative eccentricity ε from the Sommerfeld number *So* and the bearing relative length λ is based upon bisection methods in the interval $0 \leq \varepsilon \leq 1$, both in the numerical and analytical calculations. The program plots 3D graphs of pressure force field (expressed in force units) and friction force field (in percentages).

The second (EHL) module calculates the polymer bearing elastic deflection based on the Hamrock and Dowson elastohydrodynamic lubrication analysis of isoviscous-elastic body lubrication regimes.

Computational models have been verified and validated on the basis of real data for stern tube bearing operating temperatures obtained by measurements in two types of ships (a bulk carrier and a container ship).

Verification of the bearing numerical calculation procedure has been performed by the mentioned two computer programs described in [7]. Validation is based upon actual bearing temperatures for different operating regimes obtained from two actual ships in service (the bulk carrier of 50000 DWT and the container ship of 11000 TEU).

Two different bearing materials were considered in the validation calculations: a white metal tin based alloy and a polyether-based thermoplastic polyurethane. Table 2 presents the design parameters for the white metal and for the polymer aft stern tube bearing of the bulk carrier and the container ship, respectively.

Table 2 Design parameters for the white metal and polymer aft stern tube bearing of the bulk carrier and the container ship

Description	*Parameters*	*Dimensions*	*White metal bearing*		*Polymer bearing*	
			Bulk carrier	*Container ship*	*Bulk carrier*	*Container ship*
Bearing nominal diameter	D_B	mm	469.8	991.2	516.59	1072.92
Bearing length	L	mm	950	2030	1030	2140
Bearing diametrical clearance	Z	mm	0.8	1.2	1.59	2.92
Journal diameter	D_j	mm	469	990	515	1070
Lubricant (oil) viscosity	η	Pas	0.15925	0.15925	0.00088	0.00121
Bearing radial load	F_r	kN	225	1325	225	1325
Arc bearing angle	Ω_0	°	360	360	360	360

Based upon the results of the shafting elastic line, obtained from the shafting alignment calculation, the constant aft bearing radial load is 225 kN for the bulk carrier and 1325 kN for the container ship. Parameters of lubrication oil in both ships are: oil viscosity class ISO VG100, oil density ρ=910 kg/m³, kinematic viscosity at average operating temperature 30°C, ν= 176 mm²/s (dynamic viscosity of $159.25\cdot10^{-3}$ Pas) and specific heat capacity of 1922 J/kgK.

Table 3 and Table 4 show the data experimentally obtained during sea trials.

Table 3 Data of stern tube bearing operating temperature obtained from a bulk carrier of 50000 DWT

Shaft revolution	rpm	30	50	79.8	90.1	107.2	115.6	123
Bearing inlet oil temperature	°C	30	30	30	30	30	30	30.5
Effective bearing temperature	°C	32	33.5	35.5	36.5	37.5	38	39
Oil pressure in stern tube	MPa	0.12	0.12	0.12	0.12	0.12	0.12	0.12

Table 4 Data of stern tube bearing operating temperature obtained from a container ship of 11000 TEU

Shaft revolution	rpm	59	70	79	86	96	105	109
Bearing inlet oil temperature	°C	26.5	27.1	38	37	36	36	38
Effective bearing temperature	°C	28	29	40.3	39.4	39	39.4	42
Oil pressure in stern tube	MPa	0.38	0.34	0.34	0.38	0.37	0.38	0.34

4. Results and Discussion

4.1 Calculation of bearing pressure field and power loss

The calculated eccentricity ratio, bearing pressure field and power loss in the white metal stern tube aft bearing for the bulk carrier of 52000 DWT are presented in Fig. 2, whereas the calculation results for the container ship of 11000 TEU are presented in Fig. 3.

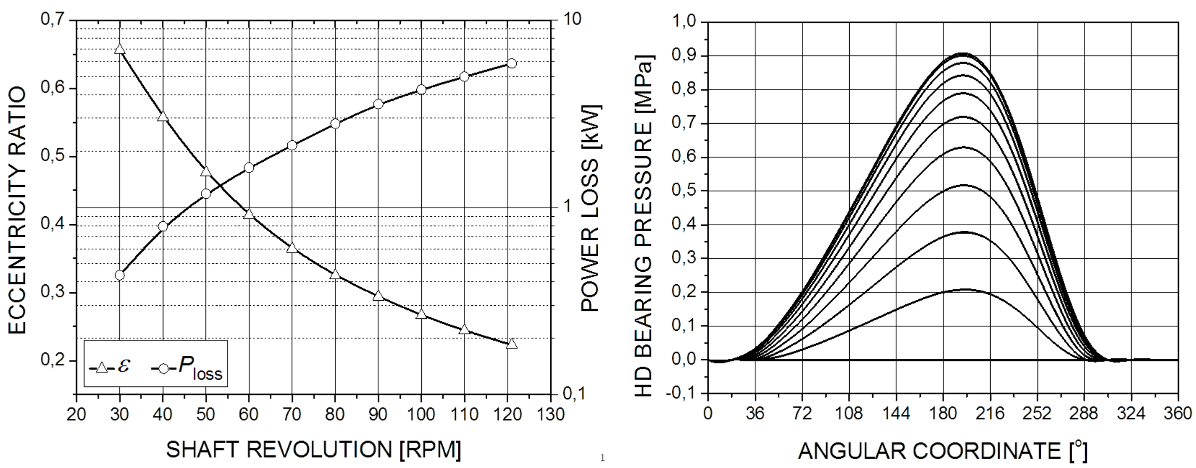

(a) (b)

Fig. 2 Calculated relationship between significant parameters of the stern tube white metal bearing in steady state conditions with constant radial load of 225 kN at various shaft revolutions: **(a)** power loss versus eccentricity ratio, **(b)** bearing pressure field at 121 rpm of the propeller shaft.

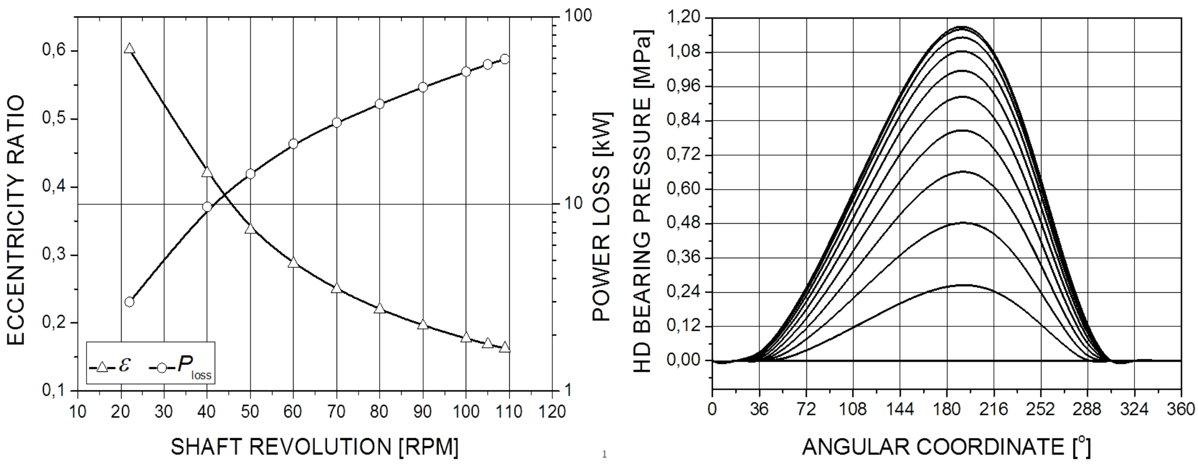

(a) (b)

Fig. 3 Calculated relationship between significant parameters of the stern tube white metal bearing in steady state condition with constant radial load of 1325 kN at various shaft revolutions: **(a)** power loss versus eccentricity ratio, **(b)** bearing pressure field at 109 rpm of the propeller shaft

Fig. 4 and Fig. 5 show the calculated results of eccentricity ratio, power loss and bearing pressure field for the bulk carrier and for the container ship with polymer bearings applied instead of white metal ones. The proposed stern tube bearing polymer material is a thermoplastic polyurethane elastomer with Young's modulus of 253 MPa [9]. In general, this type of bearing would be sea water lubricated. For the calculation, the assumed average sea water density is 1025 kg/m^3 at an average temperature of 15^{o}C, considering the trading area of the actual ships. In this condition, the sea water used as lubricant has the kinematic viscosity of 1.1843 mm²/s and the dynamic viscosity of $1.21 \cdot 10^{-3}$ Pas.

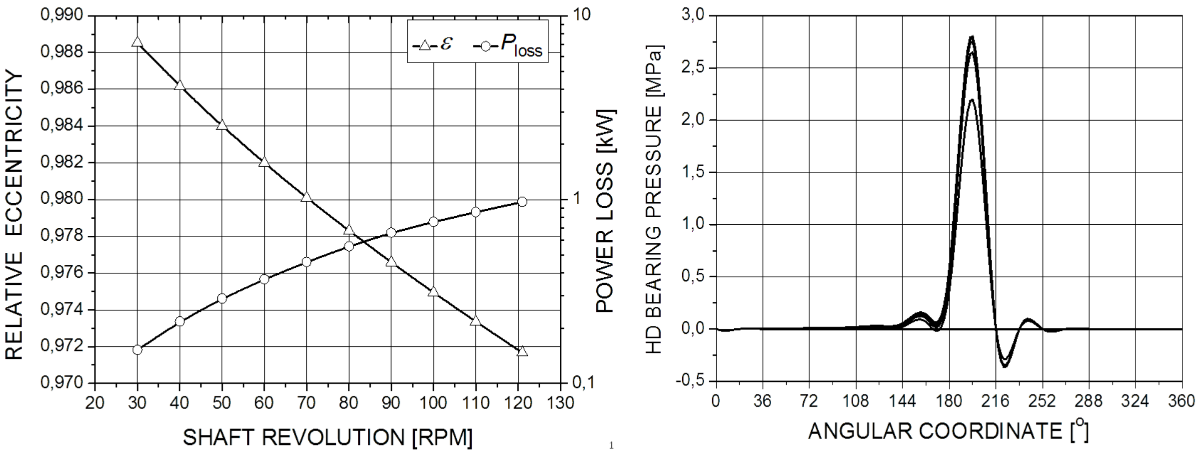

a) b)

Fig. 4 Calculated relationship between significant parameters of the stern tube with polymer bearing in steady state condition with constant radial load of 225 kN at various shaft revolutions as follows: **(a)** power loss versus eccentricity ratio, **(b)** bearing pressure field at 121 rpm of the propeller shaft.

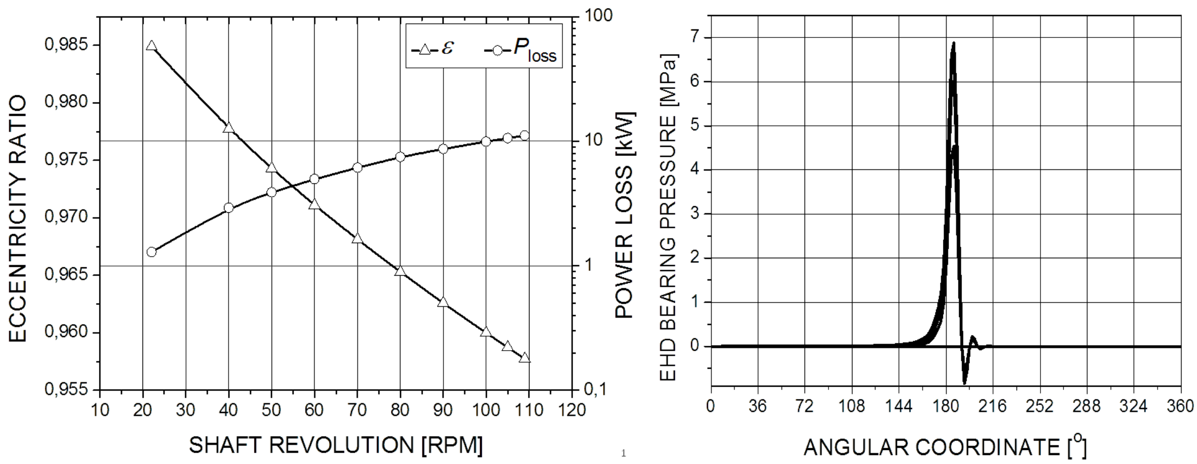

a) b)

Fig. 5 Calculated relationship between significant parameters of the stern tube with polymer bearing in steady state condition with constant radial load of 1325 kN at various shaft revolutions as follows: **(a)** power loss versus eccentricity ratio, **(b)** bearing pressure field at 109 rpm of the propeller shaft

Using the *S11isoviscRJB* software module, the elastic deflection of polymer bearing under the influence of bearing constant load is calculated. The calculation procedure is divided into three steps. The first step calculates the effective bearing diameter (after bearing deformation) together with the effective diameter clearance and the effective mean eccentricity ratio. In the second step, the *S11partialRJB* program calculates the frictional coefficient in the bearing lubricant fluid (seawater). Finally, in the third step, the calculation of the power loss $P_{loss} = f(\mu, F_r, U_j)$ in the polymer bearing at different regimes of ship propeller shaft revolutions is done.

4.2 Model validation

Prior to its validation, the computational procedure was verified by comparing the numerical calculation results with the values from the mentioned DIN standard for HL [6], and with the results from literature for EHL. After that, the computational model was validated by means of experimentally obtained data for the stern tube bearing operating temperature measured in the two types of ships: the bulk carrier of 50000 DWT and the container ship of 11000 TEU, both with white metal bearings. Namely, it is well known that the bearing temperature is the only operating parameter of the aft stern tube bearing that can actually be monitored for the ship in operation (sailing at sea). A self-developed software *S11LubeFlowRateRJB* for the calculation of lubricant oil flow and heat generated in the bearing has been implemented in order to take the aft stern tube bearing operating temperature into consideration [7]. This program calculates the lubricant flow rate from the bearing internal pressure, lubricant flow rate (from feeding pressure) and the generated heat in the bearing (based upon power loss).

Tables 5 and 6 present the results of validation. These are obtained by comparing theoretical calculations done by using the *S11partialRJB* software with the results obtained during sea trials of the bulk carrier (Table 5) and the container ship (Table 6), respectively.

Table 5 Results based on theoretical calculations done by using *S11partialRJB* and the calculation based on data from the bulk carrier ship and done by using the *S11LubeFlowRateRJB* software

rpm	Calculated ε	Calculated P_{loss} [W]	Power loss based on sea trial data P_{loss} [W]	Difference [%]
30	0.656	434	474	+9.2
50	0.476	1182	1188	+0.5
79.8	0,327	2776	2707	-2.5
90.1	0.293	3602	3543	-1.6
107.2	0.250	4780	4745	-0.7
115.6	0.233	5431	5406	-0.5
123	0.220	6045	6067	+0.4

Table 6 Results based on theoretical calculations done by using *S11partialRJB* and the calculation based on data from the container ship and done by using the *S11LubeFlowRateRJB* software

rpm	Calculated ε	Calculated P_{loss} [W]	Power loss based on sea trial data P_{loss} [W]	Difference [%]
59	0.292	20639	21162	+2.5
70	0.249	27270	27200	-0.3
79	0.223	33512	33317	-0.6
86	0.205	38874	38752	-1.9
96	0.185	47298	47859	+1.2
105	0.169	55653	56118	+ 0.8
109	0.1635	59617	60208	+ 1.0

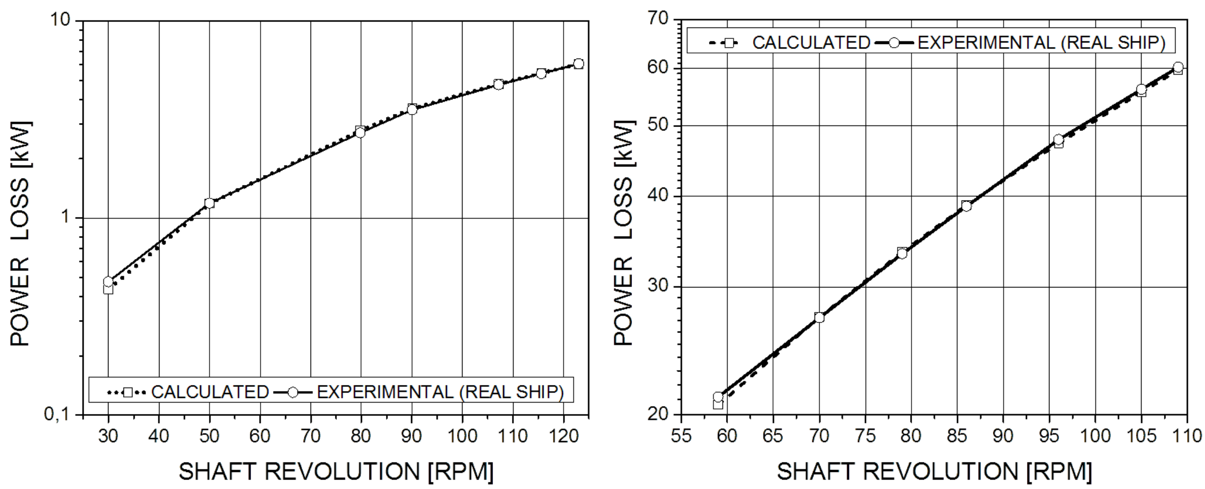

(a) (b)

Fig. 6 Comparison of the theoretical and experimental calculation of the power loss in aft stern tube white metal bearing at various shaft revolutions and constant bearing load: **(a)** bulk carrier of 50000 DWT, bearing load of 225 kN; **(b)** container ship of 11000 TEU, bearing load of 1325 kN.

Fig. 6 presents a comparison between the theoretical and the experimental calculation of power loss at different shaft revolutions for aft stern tube white metal bearings for the bulk carrier of 50000 DWT and the container ship of 11000 TEU.

4.3 Discussion of the results

Table 5 and Fig.6(a) prove that the applied calculation method is precise enough with a maximum deviation of 9.2% at the minimum speed of 30rpm, which is really insignificant.

Table 6 and Fig.6(b) show even better agreement. It is evident that the applied calculation method is precise enough with a maximum deviation of 2.5% at the minimum speed of 22rpm.

In both examples, the cause of higher deviation at lower speeds can be found in the shorter time available for the bearing thermal stabilisation at these speeds. In both cases a high degree of agreement between theoretical and experimental results at higher speeds, at which ships actually operate most of the time, has been found. This confirms that the applied calculation procedure is correct with a high degree of accuracy. The calculation results show that metallic bearings operate with a smaller value of the bearing relative eccentricity and a larger lubricant film thickness in comparison with the polymer bearings, for the same propeller shaft speed.

Comparison of the analysis results for the bulk carrier (maximal propeller shaft speed of 121 rpm and the nominal shaft diameter of 469 mm) between the white metal and the polymer stern tube bearings shows that the power loss due to friction in the polymer bearings is approximately 6 times smaller. In the case of the relatively large container ship of 11000 TEU (propeller shaft speed of 109 rpm and the nominal shaft diameter of 990 mm) a significant reduction in the power loss (approximately 5.4 times) is to be expected when polymer bearings are used instead of white metal ones.

5. Conclusions

This paper focuses on the value of friction loss in the stern tube journal bearings. Taking into consideration the fact that most of the time, stern tube bearings operate under a hydrodynamic lubrication regime in which the friction is determined by the viscosity of the lubricant, the essential operating parameters for white metal and polymer stern tube bearings have been analysed and compared. Therefore, a significant reduction in the system power loss is mostly achieved using a lubricant with low viscosity, such as sea water in the case of polymer bearings. As water-lubricated polymer bearings operate in two different lubrication regimes (i.e. HL and EHL), the bearing elastic deformation had to be taken into account in the numerical model.

The developed software consists of two modules: *S11partialRJB* and *S11isoviscRJB* described in Chapter 4. The first module is used for a hydrodynamic analysis of radial journal bearings with a length-to-diameter ratio of $1/3 \leq \lambda \leq 3$. The second module calculates the polymer bearing elastic deflection based on the Hamrock and Dowson elastohydrodynamic lubrication analysis of isoviscous-elastic body lubrication regimes.

Calculations based upon the finite difference method and the isoviscous model were validated using data collected from two different types of vessels in exploitation.

The successful validation of the model indicates that the developed software application programs attain high approximation accuracy of the actual state of the stern tube journal bearings. This also proves that the tribological HL and EHL models, based upon rather simple numerical models, can successfully be implemented to solve real world problems such as the behaviour of ship shafting bearings. Implementation of these models can lead even to a solid basis to propose a different design approach to ship designers: polymer bearings instead of white metal bearings. A deeper insight into this matter will be a matter of further work.

Nomenclature

a	contact area half-length [m]
b	contact area half-width [m]
c	radial clearance [m]
c_{eff}	effective radial bearing clearance in deformed bearing [m]
c_v	specific heat capacity of the lubricant [J/kgK]
d_H	lubricant feed hole diameter [m]
D_{Beff}	effective diameter of deformed bearing [m]
e	eccentricity [m]
E_B	Young's modulus of the bearing [GPa]
E_j	Young's modulus of the journal [GPa]
E_{red}	reduced Young's modulus [-]
F_r	bearing radial load [N]
$\tilde{F}_r$	non-dimensional bearing radial load [-]
F_t	friction force [N]
F_v	parameter for journal bearing
$\tilde{F}_t$	non-dimensional friction force [-]
$\tilde{F}$	Petroff multiplier [-]
G	parameter for journal bearing
G_E	non-dimensional elasticity parameter [-]
h	local film thickness [m]
h_c	central film thickness in deformed bearing [m]
h_{max}	maximal lubricant film thickness [m]
h_{min}	minimal lubricant film thickness [m]
h_{eff}	effective lubricant film thickness [m]
$\tilde{h}$	non-dimensional local film thickness [-]
$\tilde{H}_{min}$	non-dimensional min. film thickness [-]
$\tilde{H}_c$	non-dimensional central thickness [-]
k	non-dimensional ellipticity parameter [-]
L	bearing axial length [m]
M_v	Vogelpohl parameter [-]
n	shaft revolution speed [s^{-1}]
n_H	number of lubricant feed holes [-]
p	lubricant local pressure [Pa]
p_E	lubricant feed pressure [Pa]
$\tilde{p}$	non-dimensional lubricant pressure [-]
P_{loss}	power loss in the bearing[W]
P_{th}	friction power loss[W]
R_B	bearing radius [m]
R_j	journal radius [m]
Q	total lubricant flow rate [m^3/s]
Q_1	lubricant flow rate resulting from development of internal pressure [m^3/s]
Q_2	lubricant flow rate resulting from feed pressure [m^3/s]
q	relative lubricant flow rate [-]
R_{red}	reduced radius [m]
So	Sommerfeld number [-]
T_{in}	bearing inlet lubricant temperature [°C]
T_{out}	bearing outlet lubricant temperature [°C]
v_j	journal velocity [m/s]
U_{red}	non-dimensional speed parameter [-]
W	non-dimensional load parameter [-]
x,y	global hydrodynamic film coordinate [m]
Z	bearing diametral clearance [m]
Z_{eff}	effective diametral bearing clearance for deformed bearing [m]
ε	eccentricity ratio [-]
λ	length-diameter ratio
η	lubricant dynamic viscosity [Pas]
θ	circumferential angular coordinate [°]
θ_0	position of minimum film thickness [°]
μ	coefficient of friction [-]
ν	kinematic viscosity [mm^2/s]
υ_B	Poisson's ratio of the bearing material [-]
υ_j	Poisson's ratio of the journal material [-]
ρ	density of lubricant [kg/m^3]
τ	shear stress [Pa]
$\tilde{\tau}$	non-dimensional shear stress [-]
ψ	bearing to journal relative clearance [-]
Ω_0	arc bearing angle [°]
ω	angular velocity of journal [s^{-1}]

Acknowledgements

The results presented in the paper have been obtained in the scientific research project No. 250-2502209-2364 supported by the Ministry of Science, Education and Sport of the Republic of Croatia. We are particularly grateful to the Shipping Companies Jadroplov-Split and CMA-CGM- Marseille as well as the Brodotrogir Shipyard that have provided technical input of model test results. Support from Brazilian Research Agency CNPq – *Conselho Nacional de Desenvolvimento Tecnológico* from Liane Roldo is gratefully acknowledged.

REFERENCES

[1] Litwin W. Influence of main design parameters of ship propeller shaft water-lubricated bearings on their properties. Polish Maritime Research 4(67)2010 Vol 17; pp 39-45, Gdańsk University of Technology, Poland, 2010

[2] Stachowiak GW, Batchelor AW. Engineering Tribology. 3rd edition, Burlington: Elsevier Butterworth-Heinemann, 2005.

[3] Hamrock BJ, Schmid SR, Jacobson BO. Fundamentals of Fluid Film Lubrication –second edition, Marcel Dekker, Inc, New York-Basel,2004.

[4] Hirani H, Verma M. Tribological study of elastomeric bearing for marine propeller shaft system. Tribol Int 2009, 42: 378-390.

[5] Gruen F, Gódor I, Eichles W. Tribological test engineering – comparison of component tests of sliding bearings with tribological model tests. FAMENA issue 1, volume 30, Zagreb 2006

[6] DIN 31652-2:1983. Plain bearings - Hydrodynamic plain journal bearings designed for operation under steady-state conditions - Part 2: Functions necessary when designing circular cylindrical bearings, DIN Deutsches Institut für Normung, Berlin, 1983

[7] Komar, I. Contribution to the selection methodology of the most convenient marine propulsion stern tube bearings, Ph.D thesis, Faculty of Maritime Studies, Rijeka, 2012

[8] Vulić N, Šestan A, Cvitanić V. Modelling of propulsion shaft line and shafting alignment calculation basic procedure. Brodogradnja 2008, 59: 223-227.

[9] Ginzburg BM, Tochil'nikov GD, Bakhareva EV, Anisimov AV, Kireenko OF. Polymeric Materials for Water- Lubricated Plain Bearings. Russ J Appl Chem+ 2006, 79:5:695-706.

Submitted: 05.11.2012

Accepted: 22.02.2013

doc.dr.sc. Ivan Komar, dipl.ing
Faculty of Maritime Studies,
University of Split.
Zrinsko-Frankopanska 38,
HR-21000 Split, Croatia
email: ivan.komar@pfst.hr

prof.dr.sc.Nenad Vulić, dipl.ing
Croatian Register of Shipping.
Marasoviceva 67,
HR-21000 Split, Croatia
email: drnenad.vulic@crs.hr

prof.dr.sc. Liane Roldo
Materials Department and Post-
Graduation Program in Design of Federal
University of Rio Grande do Sul
Av. Osvaldo Aranha, 99/604,
Porto Alegre, RS, 90035-190, Brazil
email: liane.roldo@ufrgs.br